EXTENDED SHALLOW WATER PREDICTION OF OVERTOPPING

J. SHIACH, C.G. MINGHAM, D.M. INGRAM AND D.M. CAUSON
Centre for Mathematical Modelling and Flow Analysis, Manchester Metropolitan University, Chester Street, Manchester, M1 5GD, UK.

T. BRUCE AND J. PEARSON
School of Engineering and Electronics, The University of Edinburgh, Kings Buildings, Mayfield Road, Edinburgh EH9 3JL, UK.

N.W.H. ALLSOP
HR Wallingford, Howbery Park, Wallingford, Oxfordshire, OX10 8BA, UK.

An existing numerical model of wave run-up and overtopping based on the shallow water equations (SWE) has been extended to model waves in deeper water using Nwogu's formulation of the Boussinesq equations. This hybrid model uses a high resolution finite volume method to solve the SWE whilst a fourth-order accurate finite difference method is used to solve the Boussinesq equations. The numerical model has been used to predict wave heights and overtopping discharges of a series of experiments that focus on violent wave overtopping. The numerical model provided good predictions for the wave heights throughout the domain with a tendency to slightly under-predict the wave heights near the boundary of the two models. The overtopping discharge volumes calculated by the model over-predict those of the physical experiment.

1. Introduction

Overtopping of coastal structures by waves represent a hazard to buildings, cars and, most importantly, people. As a result, overtopping has been extensively studied in the last 30 years in order to provide guidance for the construction of sea defences based upon field observations and physical models. In particular, violent overtopping of seawalls was the focus of the VOWS project (Violent Overtopping by Waves at Seawalls). Violent wave overtopping occurs when waves impact against seawalls throwing water up

and over the top (Fig. 1) causing the water to overtop at speeds much larger than normal pulsating overtopping.

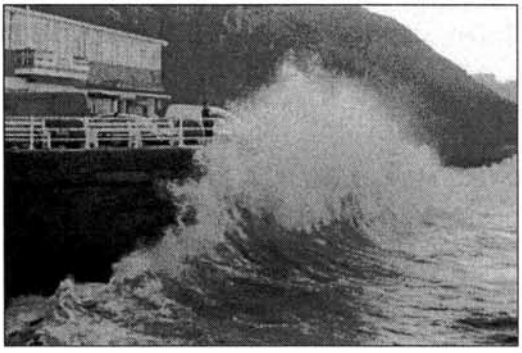

Figure 1. Violent wave overtopping event: Whitby, N. Yorks, U.K.

Previous studies include those by Franco *et al.* (1994) and Owen (1982) where data for overtopping volumes for non-breaking waves (pulsating or non-impulsive conditions) on sloping and vertical structures are presented. Goda *et al.* (1975) included violent (or impacting) conditions as well as pulsating conditions but these were not compared directly. More recently, Besley *et al.* (1998) and Pearson *et al.* (2001) have provided guidance on mean and wave-on-wave overtopping volumes under violent conditions based upon field observations and physical models.

2. Numerical Model

The use of computers has allowed the numerical solution of equations that describe fluid flow to provide engineers with an alternative to small scale physical models. These numerical models can provide coastal engineers with wave run-up and overtopping predictions without the time and cost associated with physical experiments and field observations. Ideally the full Navier-Stokes equations would provide a good choice of governing equations on which to base such a model. However, present numerical models based upon the full Navier-Stokes equations require extensive computational resources. A simplified form of the Navier-Stokes equations are the shallow water equations (SWE). Use of the SWE can drastically reduce the computation time required for a numerical model wave run-up and overtopping and therefore may represent a usable alternative to the Navier-Stokes equa-

tions.

Existing numerical models of overtopping based on the shallow water equations include HR Wallingford's ANENOME model developed by Dodd (1998) and ODIFLOCS developed by van Gent (1994) at Delft Hydraulics. ANENOME and ODIFLOCS have been used to model run-up and overtopping on shallow sloping structures (Richardson *et al.* 2002 , Clarke and Damgaard, 2002) but so far neither model has been used to model overtopping of near vertical structures. Another model based upon the SWE is AMAZON developed at the Manchester Metropolitan University (Mingham and Causon 1998 , Hu *et al.* 2000). AMAZON has been used to model overtopping of both shallow sloping structures (Hu *et al,* 2000 , Causon *et al.* 2000) and violent overtopping of near vertical structures (Shiach *et al.* 2004 , Richardson *et al.* 2001). Despite shallow water models providing good predictions of overtopping discharges for particular cases, due to the absence of terms that model dispersion, they provide poor predictions of wave propagation where the relative depth ratio (h/L, where h is the water depth and L is the wavelength) is larger than 0.05. This has been overcome previously by reducing the computational domain so that only the area immediately seaward of the structures is modelled.

To overcome this shortcoming in shallow water models, an extended form of the Boussinesq equations has been used to model wave propagation in intermediate depth water ($0.05 < h/L < 0.5$) allowing the seaward boundary of the numerical model to extended out further and therefore increase the applicability of the model. This new hybrid model has been used to provide wave run-up and overtopping discharge comparisons to the VOWS experiments performed at Edinburgh University.

The numerical model used here is a hybrid of the non-linear shallow water equations (SWE) and Nwogu's Boussinesq equations. The SWE are only applicable for a relative depth of $h/L < 0.05$ whereas Nwogu's Boussinesq equations have been shown to have a range of applicability of $0 < h/L < 0.5$ (Nwogu, 1993). However, the SWE are quicker and easier to solve than the Boussinesq equations and do not require any special treatment for the case where the bed topography is above the still water level. Therefore the numerical model uses the Boussinesq equations to model wave propagation in intermediate depth water and the SWE to model wave run-up and overtopping, i.e.,

$$\text{Numerical model} = \begin{cases} \text{Boussinesq} & \text{where } h/L > 0.05 \\ \text{SWE} & \text{elsewhere} \end{cases} . \qquad (1)$$

2.1. *The Shallow Water Equations*

The SWE are a depth-averaged form of the Navier-Stokes equations that can model breaking waves as a discontinuity in height. The SWE written in vector form are:

$$\frac{\partial}{\partial t}\mathbf{U} + \frac{\partial}{\partial x}\mathbf{F}(\mathbf{U}) + \frac{\partial}{\partial y}\mathbf{G}(\mathbf{U}) = \mathbf{\Omega} \tag{2}$$

where $\mathbf{U}$ is the vector of conserved variables, $\mathbf{F}(\mathbf{U})$ and $\mathbf{G}(\mathbf{U})$ are flux vector functions and $\mathbf{\Omega}$ is the vector of source terms that are used to model bed topography, friction and bed shear stresses. Here the terms that only model bed topography are used. The conserved, flux and source term vectors are

$$\mathbf{U} = \begin{pmatrix} \phi \\ \phi u \\ \phi v \end{pmatrix}, \quad \mathbf{F}(\mathbf{U}) = \begin{pmatrix} \phi u \\ \phi u^2 + \frac{1}{2}\phi^2 \\ \phi uv \end{pmatrix}, \tag{3}$$

$$\mathbf{G}(\mathbf{U}) = \begin{pmatrix} \phi u \\ \phi uv \\ \phi v^2 + \frac{1}{2}\phi^2 \end{pmatrix}, \quad \mathbf{\Omega} = \begin{pmatrix} 0 \\ g\phi\frac{\partial H}{\partial x} \\ g\phi\frac{\partial H}{\partial y} \end{pmatrix}. \tag{4}$$

where $\phi = gh$ is the geopotential, $g = 9.81\text{ms}^{-2}$ is the acceleration due to gravity, h is the local water depth, u and v are depth-averaged horizontal velocities in the x and y directions respectively and H is the distance between the bed surface and a fixed arbitrary datum measured downwards.

2.2. *Shallow water equations solver – AMAZON*

The SWE given in Eqs. (2)–(4) are solved using a high-resolution finite volume method that is second-order in time and space. The MUSCL-Hancock scheme is a Godunov-type method that uses a monotonic reconstruction of the conserved variables to obtain values at cell interfaces that prevent spurious oscillations in the solution. Solutions to local Riemann problems that are required for the corrector stage are calculated using the HLL approximate Riemann solver (Harten *et al.* 1983). A full description of the SWE numerical scheme including applications to well known test cases can be found in Mingham and Causon (1998) .

Previous versions of the AMAZON solver used an operator splitting technique for the treatment of the source terms. The MUSCL-Hancock scheme described above was used to solve the advection terms on the left-hand side of Eq. (2) whilst a first-order implicit Euler method was used

for the source terms. Zhou *et al.* (2001) developed a surface gradient method (SGM) for the treatment of bed source terms in the SWE that uses the water surface elevation instead of the geopotential as the basis for the linear reconstruction in the mass transport equation. This approach insures that any differences in the solution to the geopotential and the bed source terms do not have an adverse affect on the solution. The implementation of the SGM for the MUSCL-Hancock requires very little alteration to the existing scheme and the additional computational cost is negligible. A full description of the SGM and proof of its conservative properties can be found in Zhou *et al.* (2001) .

2.3. *Nwogu's Boussinesq Equations*

Nwogu (1993) derived a new form of Boussinesq equation that uses the horizontal velocity at an arbitrary depth as the dependent variable. This derivation leads to a system of equations that, by altering a free parameter α, can change the dispersive properties of the system. Nwogu's Boussinesq equations are given as:

$$\eta_t + \nabla \cdot [(h+\eta)\mathbf{u}_\alpha] + \nabla \cdot \left\{ \left(\frac{z_\alpha^2}{2} - \frac{h^2}{6} \right) h \nabla(\nabla \cdot \mathbf{u}_\alpha) + \left(z_\alpha + \frac{h}{2} \right) h \nabla[\nabla \cdot (h\mathbf{u}_\alpha)] \right\} = 0 \quad (5)$$

$$\mathbf{u}_{\alpha t} + g\nabla\eta + (\mathbf{u}_\alpha \cdot \nabla)\mathbf{u}_\alpha + z_\alpha \left\{ \frac{z_\alpha}{2} \nabla(\nabla \cdot \mathbf{u}_{\alpha t}) + \nabla[\nabla \cdot (h\mathbf{u}_{\alpha t})] \right\} = 0 \quad (6)$$

where η is the water surface elevation above the still water level (SWL), $\mathbf{u}_\alpha = (u_\alpha, v_\alpha)$ is the horizontal velocity at an arbitrary depth z_α, h is the distance between the SWL and the bed surface, $\nabla = (\partial/\partial x, \partial/\partial y)$ is the horizontal gradient operator and $g = 9.81\text{ms}^{-2}$ is the acceleration due to gravity.

The value of the free parameter α gives the depth z_α at which the horizontal velocities are calculated (using the SWL as the basis for the coordinate system), and also determines the dispersive properties of the system. The free parameter can take a value in the range $-1/2 \leq \alpha \leq 0$ where $\alpha = -1/2$ corresponds to the velocities at the bed surface and $\alpha = 0$ corresponds to velocities at the free surface (a value of $\alpha = -1/3$ gives the standard form of the Boussinesq equations derived by Peregrine, 1967). Nwogu (1993) obtained a value of $\alpha = -0.390$ (corresponding to a depth of $z_\alpha = -0.531h$) by minimising the error between the dispersion properties of the linearised system and linear dispersion theory.

2.4. *Boussinesq Equations Solver*

Nwogu's Boussinesq equations are solved using a fourth-order accurate finite-difference method described by Wei and Kirby (1995) . Integration through time is achieved by a third-order Adams-Bashforth predictor and fourth-order Adams-Moulton corrector method. All first-order derivatives are discretised using a fourth-order stencil insuring that the order of the truncation error in the numerical scheme is less than that of the order of the error in the derivation of the governing equations. The momentum equation is written so that all terms including time derivatives are collected together resulting in a tri-diagonal system that requires solving at each time step.

2.5. *Wave Generation*

Wave generation within the Boussinesq domain is achieved by use of an internal source function method. Larsen and Dancy (1983) first used the method where mass is added to the continuity equation at single point in the solution domain. The method works well when a staggered mesh is used, but applying this method to a scheme that uses a collocated mesh causes the scheme to become unstable. To overcome this, Wei *et al.* (1999) used a Gaussian shape function to add the mass over a range of mesh points so that the scheme remains stable.

Mass is added to Eq. (5) in the form of a source function defined by

$$f(x,t) = g(x)s(t) \tag{7}$$

where $s(t)$ is the input time series and $g(x)$ is the Gaussian shape function given as

$$g(x) = \exp\left[-\beta(x - x_s)^2\right] \tag{8}$$

where x_s is the centre of the source function and β is a parameter that determines the width of the source function. It is beneficial to use a narrow source function when generating waves within the Boussinesq domain as addition nodes are required for the source function. Here the authors have chosen a source function width that is half the wavelength of a typical wave, L, determined by the peak wave period. This leads to the following definition of β

$$\beta = \frac{80}{L^2}. \tag{9}$$

The amplitude of the Gaussian shape function is given as

$$D = \frac{2a(\omega^2 - \alpha_1 g k^4 h^3)}{\omega k I[1 - \alpha(kh)^2]} \tag{10}$$

where a is the amplitude of the input signal, ω is the peak frequency, $\alpha_1 = \alpha + 1/3$, k is the wavenumber, h is the water depth and I is given by

$$I = \sqrt{\frac{\pi}{\beta}} \exp\left(\frac{-k^2}{4\beta}\right). \tag{11}$$

2.6. *Boundary Conditions*

There are three types of boundary condition used in the hybrid numerical model: absorbing boundary for the Boussinesq domain, incident wave boundary condition for the SWE domain and transient boundary condition for the SWE domain. A sponge layer analogy is used to provide absorbing boundaries for the Boussinesq domain. The boundary conditions for the SWE domain are described in Shiach *et al.* (2004) .

3. Results

The numerical model described in Section 2 has been used to model physical experiments carried out at Edinburgh University's wave flume facility. The experiments were carried out as part of the EPSRC funded VOWS project whose aim was the study of violent wave overtopping (Allsop *et al.* 2005) . The experiment consisted of an 11.21 metre wave flume with a still water level (SWL) of 0.7 metres (Fig. 2). The bathymetry for the experiment modelled here consists of a 1:10 sloping beach on which a near vertical 10:1 battered wall is located so that the water height at the toe of the wall is 0.09 metres. The crest freeboard is 0.15 metres. Gauges are placed at 1.0, 2.0, 3.0, 4.25, 5.5, 6.75, 8.0 and 11.21 metres from the battered wall recording water depth, an overtopping detector is placed on top of the wall to record overtopping events and a tank connected to a load cell is placed behind the battered wall to calculate discharge volume. An absorbing flap-type wave generator is used to generate waves from the JONSWAP spectrum with a peak enhancement parameter of $\gamma = 3.3$. As the waves propagate towards the battered wall, the sloping beach causes them to shoal and break upon the structure therefore causing violent overtopping to occur.

Comparisons of the water surface elevation for the seven depth gauges are given in Fig. 3. The water surface height generated by the numerical

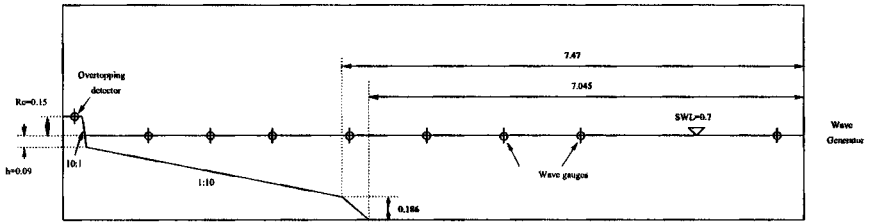

Figure 2. Sketch of the Edinburgh wave flume.

model shows good agreement with the physical water surface for the gauges close to the wave generator. For the gauges placed 4.25 and 3.0 metres from the battered wall, the numerical model tends to under-predict the wave heights. This is probably due to the absence of flow from the SWE domain into the Boussinesq domain. The depth gauges placed within the SWE domain give good agreement with the physical experiment.

The significant wave heights (H_s = mean of the top 1/3 wave heights) for the Edinburgh experiments and the numerical model are contained in Tables 1 and 2 respectively. This data can also be seen in the form of a scatter plot in Fig. 4 where the experimental values of H_s are plotted against the numerical predictions of H_s. The numerical model provides wave height predictions to within 10% of the experimental wave heights, although they tend to under-predict them. This is probably due to the fact that waves are not reflected back into the Boussinesq domain.

Table 1. Significant wave heights (m) for each of the depth gauges over runs 16 – 21 of the Edinburgh experiments.

	Gauge distance from wall in metres						
Run	8.0	6.75	5.5	4.25	3.0	2.0	1.0
16	0.069	0.070	0.072	0.072	0.066	0.064	0.060
17	0.086	0.086	0.088	0.089	0.082	0.082	0.076
18	0.078	0.078	0.081	0.079	0.072	0.082	0.096
19	0.102	0.102	0.105	0.102	0.094	0.096	0.125
20	0.085	0.084	0.084	0.080	0.080	0.075	0.078
21	0.099	0.088	0.096	0.097	0.095	0.089	0.087

The mean overtopping discharges (q = l/s m) for runs 16 – 21 can be seen in Table 3. For all of the runs of the experiments compared here, the numerical model over-predicts the volume of water overtopping the seawall. In order to compare the overtopping discharges for the different experimental set-ups, dimensionless parameters for the volume of discharge

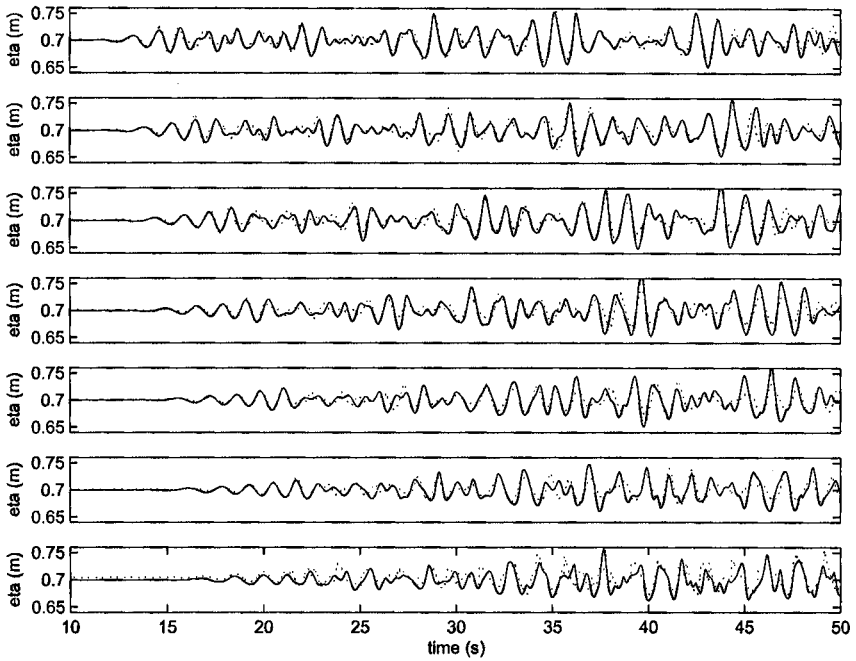

Figure 3. Comparison between the experimental water surface (solid line) and the numerical water surface (dotted line) for the gauges placed (from top to bottom) 8.0, 6.75, 5.5, 4.25, 3.0, 2.0 and 1.0 metres from the seawall.

Table 2. Significant wave heights (m) for each of the depth gauges over runs 16 – 21 of the numerical model.

	Gauge distance from wall in metres						
Run	8.0	6.75	5.5	4.25	3.0	2.0	1.0
16	0.071	0.067	0.063	0.058	0.055	0.056	0.062
17	0.089	0.084	0.079	0.073	0.072	0.072	0.077
18	0.076	0.071	0.067	0.063	0.060	0.059	0.086
19	0.097	0.093	0.086	0.081	0.080	0.080	0.108
20	0.092	0.089	0.087	0.075	0.073	0.070	0.065
21	0.110	0.105	0.101	0.089	0.087	0.085	0.076

and freeboard have been calculated (Besley, 1999) . These are compared with the empirical formula for the dimensionless overtopping discharge for vertical structures derived by Besley in Fig. 3. Where $0.05 < R_h < 0.1$ the numerical model provides good agreement with the Besley curve, but

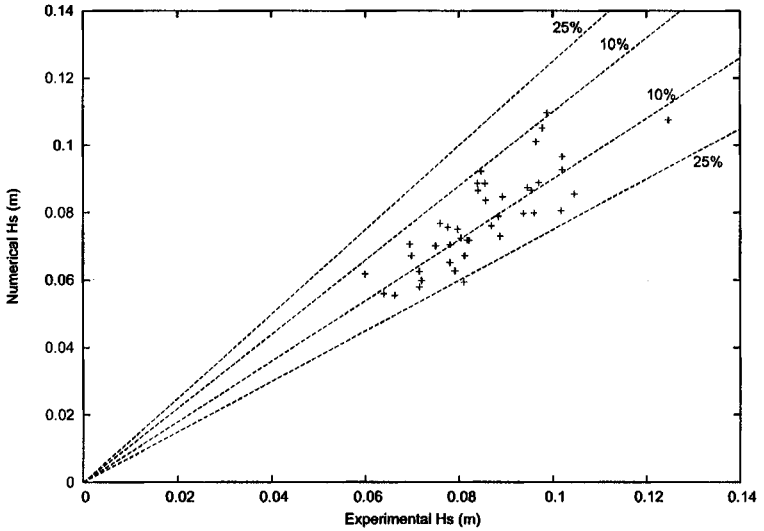

Figure 4. Significant wave heights: Comparison between the VOWS experiments and the numerical model.

where the dimensionless freeboard increases to approximately 0.2 there is a notable different between the discharge values from the numerical model and both the Besley curve and the experimental values.

Table 3. Mean overtopping volumes (q = l/s m).

Run	Experiment	Numerical Model
16	0.0056	0.0356
17	0.0275	0.0338
18	0.0213	0.0525
19	0.0481	0.0725
20	0.0119	0.0069
21	0.0219	0.0725

4. Conclusions

A hybrid numerical model based on the shallow water equations and Nwogu's extended Boussinesq equations has been presented. A second-order finite-volume method was used to solve the shallow water equations incorporating the Surface Gradient Method for the treatment of source

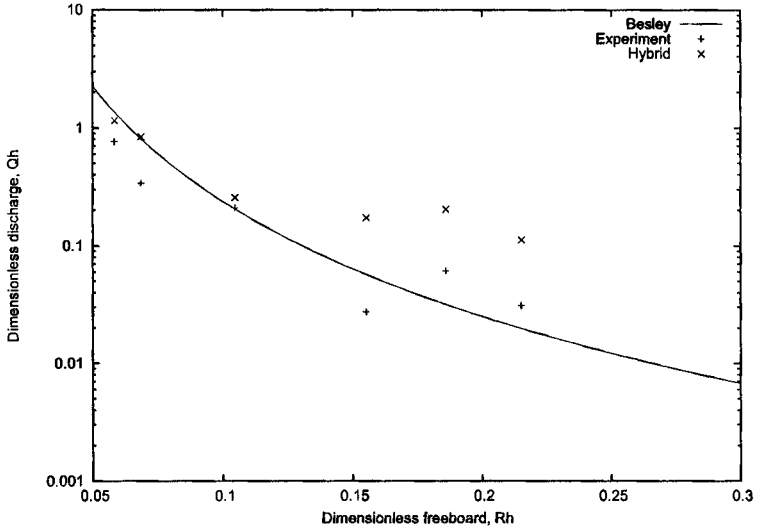

Figure 5. Dimensionless discharge (Q_h) plotted against dimensionless freeboard (R_h) for the physical model and the numerical model.

terms. The extended Boussinesq equations were solved using a fourth-order finite-difference method where the truncation error in the numerical scheme is less than that of the governing equations, thus ensuring that the dispersive properties of the governing equations are fully retained in the model. Wave generation was achieved by using an internal source function method within the Boussinesq domain using wave heights from the physical experiments.

The numerical model was used to give comparisons of water surface elevation and mean overtopping discharge to a series of experiments carried out to model violent wave overtopping of a near vertical seawall. The numerical model provided good predictions of the water surface elevation for locations throughout the flume. The significant wave heights were calculated for comparison and, whilst most values were accurate to within 10%, there was a general trend for the numerical model to under-predict the wave heights. The mean overtopping discharge volume was over-predicted by the numerical model in all 6 runs modelled here. It is suspected that the under-prediction of the wave heights for the gauges located near the boundary between the Boussinesq domain and the shallow water domain is a result of the absence of reflective waves entering the Boussinesq domain. Further work to rectify this problem is being undertaken.

Acknowledgments

The authors are grateful for the funding provided for the VOWS and CLASH projects. The VOWS project was funded by the EPSRC under two linked grants, numbers GR/M 42312 and GR/M 42428. The CLASH project was funded by the EU, contract number EVK3-CT-2001-00058.

References

1. N.W.H. Allsop, T. Bruce, J. Pearson, and P. Besley. Wave overtopping at vertical and steep seawalls. *ICE Water, Maritime and Engineering Journal*, In Press.
2. P. Besley. Overtopping of seawalls - design and assessment manual. R&D Technical Report W178. Technical Report 1 85705 069 X, Environmental Agency, Bristol, 1999.
3. P. Besley, T. Stewart, and N.W.H. Allsop. Overtopping of vertical structures: new methods to account for shallow water conditions. In *Proceedings of International Conference on Coastlines, Structures and Breakwaters '98*, pages 46–57. Institution of Civil Engineers, 1998.
4. D.M. Causon, D.M. Ingram, C.G. Mingham, J. Zang, K. Hu, and J. Zhou. Numerically simulating seawall overtopping. In Billy L. Edge, editor, *Coastal Engineering 2000*, volume 3. ICCE, ASCE, 2000.
5. S. Clarke and J. Damgaard. Applications of a numerical model of swash zone flow on gravel beaches. In Billy L. Edge, editor, *Coastal Engineering 2002*, volume 1, pages 1028–1036, Cardiff, 2002.
6. N. Dodd. A numerical model of wave run-up, overtopping and regeneration. In *Proceedings ASCE Journal of Waterways, Port and Coastal Engineering*, volume 124, pages 73–81. ASCE New York, 1998.
7. L. Franco, M. de Gerloni, and J. van der Meer. Wave overtopping on vertical and composite breakwaters. In *Proceedings from 24th International Conference on Coastal Engineering*, Kobe, 1994.
8. Y. Goda, Y. Kishira, and Y. Kamiyama. Laboratory investigation on the overtopping rates of sea walls by irregular waves. *Ports and Harbour Research Institute*, 14:3–44, 1975.
9. K. Hu, C.G. Mingham, and D.M. Causon. Numerical simulation of wave overtopping of coastal structures using the non-linear shallow water equations. *Coastal Engineering*, 41:433–465, 2000.
10. J. Larsen and H. Dancy. Open boundaries in short wave simulation. *Coastal Engineering*, 7:285–297, 1983.
11. C.G. Mingham and D.M. Causon. High-resolution finite-volume method for shallow water flows. *Journal of Hydraulic Engineering*, 124:605–614, 1998.
12. O. Nwogu. An alternative form of the Boussinesq equations for nearshore wave propagation. *Journal of Waterway, Port, Coastal, and Ocean Engineering*, 119(6):618–638, 1993.
13. M. Owen. Overtopping of sea defences. In *Proceedings from Conference Hy-*

draulic Modelling of Civil Engineering Structures, pages 469–480, Coventry, 1982. BHRA.

14. J. Pearson, T. Bruce, and N.W.H. Allsop. Prediction of wave overtopping at steep seawalls – variabilities and uncertainties. In *Proceedings Waves '01*, San Francisco, 2001. ASCE.
15. D.H. Peregrine. Long waves on a beach. *Journal of Fluid Mechanics*, 27(4):815–827, 1967.
16. S.R. Richardson, D.M. Ingram, C.G Mingham, and D.M. Causon. On the validity of the shallow water equations for violent overtopping. In Billy L. Edge and J. Michael Hemsley, editors, *Ocean Wave Measurement and Analysis*, volume 2, pages 1112–1124. Waves 2001, ASCE, 2001.
17. S.R. Richardson, T. Pullen, and S. Clarke. Jet velocities of overtopping waves on sloping structures: measurements and computation. In Billy L. Edge, editor, *ICCE 2002*, volume 2, pages 2239–2250, Cardiff, 2002.
18. J.B. Shiach, C.G. Mingham, D.M. Ingram, and T. Bruce. The applicability of the shallow water equations for modelling violent wave overtopping. *Coastal Engineering*, 51:1–15, 2004.
19. M.R.A. van Gent. Modelling of wave action on and in coastal structures. *Coastal Engineering*, 22, 1994.
20. G. Wei and J.T. Kirby. Time-dependent numerical code for extended Boussinesq equations. *Journal of Waterway, Port, Coastal, and Ocean Engineering*, 121(5):251–261, 1995.
21. G. Wei, J.T. Kirby, and A. Sinha. Generation of waves in Boussinesq models using a source function method. *Coastal Engineering*, 36:271–299, 1999.
22. J.G. Zhou, D.M. Causon, C.G. Mingham, and D.M. Ingram. The surface gradient method for the treatment of source terms in the shallow water equations. *Journal of Computational Physics*, 168:1–25, 2001.